GLOBAL AEROSOL EFFECT RETRIEVAL FROM PASSIVE HYPERSPECTRAL MEASUREMENTS

M. de Graaf[1,2], L. G. Tilstra[1] and P. Stammes[1]

[1]*Royal Netherlands Meteorological Institute (KNMI), Wilhelminalaan 10, 3732 GK, De Bilt, The Netherlands*

[2]*Delft University of Technology, P.O. Box 5, 2600 AA Delft, The Netherlands*

Email: graafdem@knmi.nl

ABSTRACT

Absorbing aerosols can have a significant local direct radiative effect (DRE), while the global average aerosol DRE remains highly uncertain. Modelling studies have shown that the magnitude and sign of the aerosol DRE at the top of the atmosphere (TOA) depend on the scene, especially on the albedo of the scene under the aerosol layer. It changes with cloud fraction, from large positive for overcast conditions when aerosols are present above the cloud, to large negative for clear sky ocean scenes. Observational studies, which are necessary to constrain the model studies, have been scarce.

The results of modelling studies depend strongly on the assumed aerosol properties. Observational studies also need to assume aerosol type and geophysical properties to derive aerosol optical properties from radiation measurements. This introduces large uncertainties in the retrieved aerosol DRE. Furthermore, the retrieval of aerosols over clouds from passive instruments is difficult, due to the large optical thickness of clouds. Therefore, observational studies of aerosol direct and indirect effects from passive satellite instruments are invariably restricted to aerosol studies close to the cloud edges. We have developed a method to derive the aerosol DRE for smoke over clouds directly from passive satellite hyperspectral reflectance measurements, independent of aerosol microphysical property assumptions. This allows us to assess the local aerosol DRE from passive imagery directly on a pixel to pixel basis, even over clouds.

The solar radiative absorption by smoke layers is quantified using the TOA reflectance spectrum from the ultraviolet (UV) to the shortwave infrared (SWIR). UV-absorbing aerosols have a strong signature that can be detected using UV reflectance measurements. Since the aerosol extinction optical thickness decreases rapidly with increasing wavelength for smoke, the properties of the scene below the aerosol layer can be retrieved in the SWIR, where aerosol extinction optical thickness is sufficiently small. Then, using radiative transfer computations, the contribution of the scene to the reflected radiation can be modelled for the entire solar spectrum. In this way, aerosol effects can be separated from all other effects in a scene. Aerosol microphysical assumptions and retrievals are avoided by modelling only the aerosol-free scene spectra. All the aerosol effects are in the reflectance measurements. The method works especially well for bright scenes, e.g. scenes with clouds underlying the absorbing aerosol layer.

In an initial study, supported by ESA within Support To Science Element, an algorithm was developed to derive the aerosol DRE over marine clouds, using the spectrometer SCIAMACHY, which produced shortwave reflectance spectra from 2002 till 2012. The reflectance spectra from SCIAMACHY are ideally suited to study the effect of aerosols on the entire shortwave spectrum. The algorithm has been improved and adapted to suit data from any instrument, or a combination of instruments, that measures UV, visible and SWIR reflectances at TOA simultaneously. Examples include OMI and MODIS, flying in the A-Train constellation, and TROPOMI, on the future Sentinel 5 mission, combined with NOAA's NPP VIIRS. This would produce aerosol DRE estimates with unprecedented accuracy and spatial resolution.

We show results from SCIAMACHY and initial results from OMI/MODIS. The aerosol DRE over clouds over the South Atlantic Ocean west of Africa, averaged through August 2006 was found to be 23 ± 8 Wm^{-2} with a mean variation over the region in this month of 22 Wm^{-2}. Locally the aerosol DRE over clouds in that month was as high as 132 ± 8 Wm^{-2}, absorbing about 10% of the local incoming solar radiation.

Key words: SCIAMACHY; aerosols; clouds; radiative forcing.

1. INTRODUCTION

The radiative effects of atmospheric aerosols potentially compensate for the increases in the effects of greenhouse gases, but the magnitude and even sign of their net effect is uncertain, due to their influences on clouds [1, 2].
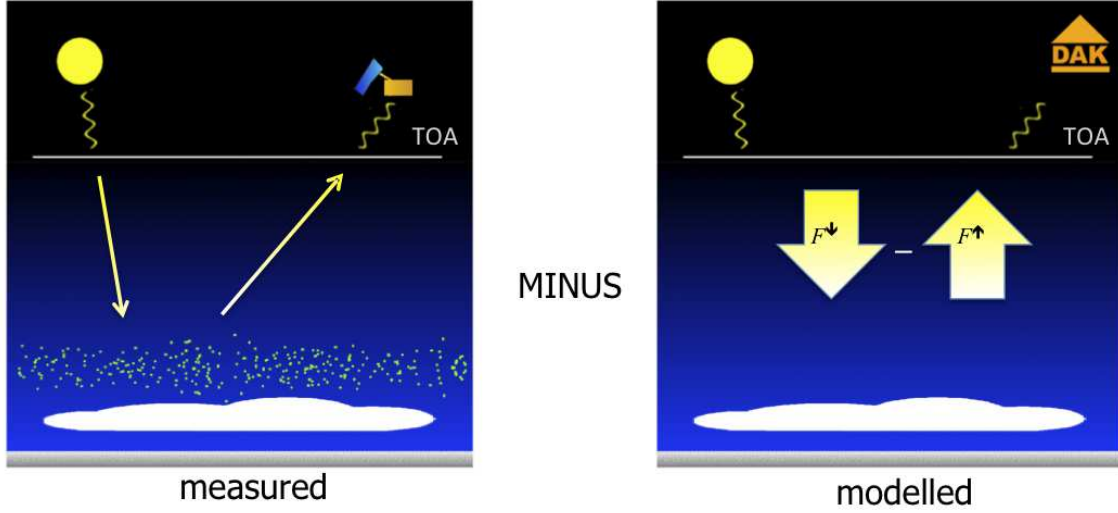
Figure 1. Illustration of the differential absorption *technique. The aerosol Direct Radiative Effect is computed using the measured upwelling radiance at TOA and compared to an equivalent simulated aerosol-free cloud scene. In this way assumptions on or retrievals of aerosol parameters are avoided.*

This makes the aerosol climate effects one of the least certain components of global climate models [3, 4]. Even the aerosol direct radiative effect (DRE), the component of aerosol climate forcing that neglects all influences on clouds, is still poorly constrained, due to the heterogeneous distribution of aerosol sources and sinks and the influence of clouds on global observations of aerosols. In particular, the characterisation of aerosol properties in cloud scenes has been proved challenging. Locally, the aerosol DRE can be very large and dominate the climate forcing.

Here, a method to quantify the aerosol DRE over clouds over the South-Atlantic Ocean is introduced. The methodology was designed to quantify the aerosol DRE from the reflectance difference of measured aerosol-polluted cloud spectra from SCIAMACHY and modelled aerosol-unpolluted cloud spectra.

2. AEROSOL DIRECT RADIATIVE EFFECT OVER CLOUDS

A radiative forcing or radiative effect of an atmospheric constituent x can be defined as the difference in the net irradiance ΔF at a certain level with and without the forcing constituent [e.g. 4, 5]:

$$\Delta F_x = F^{\mathrm{net}}_{\mathrm{with}\ x} - F^{\mathrm{net}}_{\mathrm{without}\ x}, \tag{1}$$

where the net irradiance is defined as the difference between the downwelling and upwelling irradiances,

$$F^{\mathrm{net}} = F^{\downarrow} - F^{\uparrow}. \tag{2}$$

Therefore, at the TOA, where the downwelling irradiance is the incoming solar irradiance F_0 for all scenes, the radiative effect of aerosols overlying a cloud is given by

$$\Delta F^{\mathrm{TOA}}_{\mathrm{aer}} = F^{\uparrow\ \mathrm{TOA}}_{\mathrm{cld}} - F^{\uparrow\ \mathrm{TOA}}_{\mathrm{cld}\ +\ \mathrm{aer}}, \tag{3}$$

where $F^{\uparrow\ \mathrm{TOA}}_{\mathrm{cld}}$ is the upwelling irradiance at the TOA for an aerosol-free cloud scene and $F^{\uparrow\ \mathrm{TOA}}_{\mathrm{cld}\ +\ \mathrm{aer}}$ is the upwelling irradiance for an aerosol-polluted cloud scene. By equation (3), if energy is absorbed in the atmosphere by the aerosols, the radiative forcing is positive.

The monochromatic irradiance $F(\lambda)$ can be found by integrating the monochromatic radiance $I(\lambda)$ over an entire hemisphere solid angle

$$F(\lambda) = \int_{\Omega} I(\lambda) \cos\Theta d\Omega, \tag{4}$$

which can be written in polar coordinates as

$$F(\lambda) = \frac{\mu_0 F_0(\lambda)}{\pi} \int_0^{2\pi} \int_0^1 R(\lambda, \mu, \phi; \mu_0, \phi_0) \mu d\mu d\phi, \tag{5}$$

where μ_0 is the cosine of the solar zenith angle, μ the cosine of the viewing zenith angle, and ϕ_0 and ϕ the azimuth angle of the incoming and outgoing beam relative

to the scattering plane, respectively. $\mu_0 F_0$ is the TOA solar irradiance incident on a horizontal surface unit and R is the reflectance, defined as

$$R(\lambda) = \frac{\pi I(\lambda)}{\mu_0 F_0(\lambda)}. \qquad (6)$$

The Earth's reflectance R at the TOA is the quantity measured by SCIAMACHY (first order product) and computed by a Radiative Transfer Model (RTM) for all levels. Below, R and all other quantities refer to quantities at the TOA.

The (local) plane albedo A for a scene is defined as the integral of R over all angles

$$A(\lambda, \mu_0) = \frac{1}{\pi} \int_0^{2\pi} \int_0^1 R(\lambda, \mu, \phi; \mu_0, \phi_0) \mu d\mu d\phi. \quad (7)$$

By substituting equation (7) in (5) and integrating over wavelength, the aerosol effect at the TOA (equation (3)) becomes

$$\Delta F_{\mathrm{aer}} = \int_0^\infty \mu_0 F_0 \left(A_{\mathrm{cld}} - A_{\mathrm{cld + aer}} \right) d\lambda. \qquad (8)$$

This is illustrated in Figure 1. Only the aerosol-free case is simulated, the aerosol+cloud case is taken from the measured radiances directly. For the simulated case the plane albedo can be obtained from the model results, by integrating the reflectances in all directions. However, for the measured case with clouds and aerosols, only the reflectance in the measured direction is known. Therefore, the plane albedo for this scene must be estimated.

A measure for the angular distribution of the scattering energy as a function of the scattering angle for a scene is the anisotropy factor B,

$$B = R/A. \qquad (9)$$

Assuming that the anisotropy factors are the same for the clean and polluted cloud scenes, $B_{\mathrm{cld}} = B_{\mathrm{cld + aer}}$, equation (8) can be written as

$$\Delta F_{\mathrm{aer}} \simeq \Delta F_{\mathrm{aer}}^{\mathrm{est}} = \int_0^\infty \frac{\mu_0 F_0 \left(R_{\mathrm{cld}} - R_{\mathrm{cld + aer}} \right)}{B_{\mathrm{cld}}} d\lambda. \qquad (10)$$

Equation (10) is used to derive the aerosol DRE over clouds from SCIAMACHY measurements of $R_{\mathrm{cld+aer}}$ and model results of R_{cld} and B_{cld}.
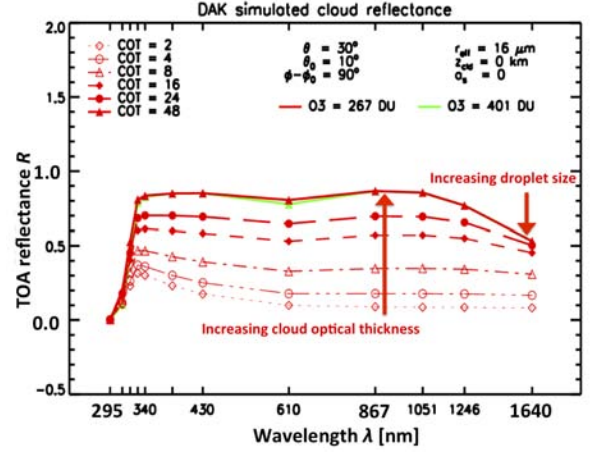

Figure 2. Example of the simulated cloud reflectances using the RTM. The parameters used for these simulations are as given. In general, the reflectance increases for increasing cloud optical thickness, due to the increased brightness of a thicker cloud. At near IR wavelengths (like 1246 nm) water droplets are absorbing, and the reflectance decreases for larger droplets, due to stronger absorption. This is the basis for the retrieval of cloud optical thickness and droplet size.

2.1. Modelled unpolluted cloud reflectance spectra

The basis for the modelling of the unpolluted cloud reflectance spectra R_{cld} is a LookUp Table (LUT) of cloud TOA reflectances at various wavelengths in the spectrum, modelled for any normal circumstances. For each measured cloud scene the necessary parameters are retrieved from the measured reflectance spectrum to search the LUT for the appropriate equivalent unpolluted cloud reflectances. The measured spectrum is then used to find the entire reflectance spectrum of the unpolluted cloud scene.

Radiative Transfer Model

The Doubling–Adding KNMI (DAK) RTM [7] was used to model the TOA reflectances. DAK computes the vectorised monochromatic reflectance and transmittance of a pseudo–spherical atmosphere, using the polarised doubling–adding method [8]. The internal radiation field of the atmosphere is determined in a finite number of layers, each of which can have Rayleigh scattering, gas absorption, and aerosol and cloud particle scattering and absorption.

A TOA reflectance LUT at various wavelengths was created for scenes with water clouds under various conditions. The atmosphere was divided in 32 layers, simulating a standard mid-latitude atmosphere gas and temperature profile [9]. The standard ground pressure was 1013 hPa. Water clouds were simulated in a one kilome-
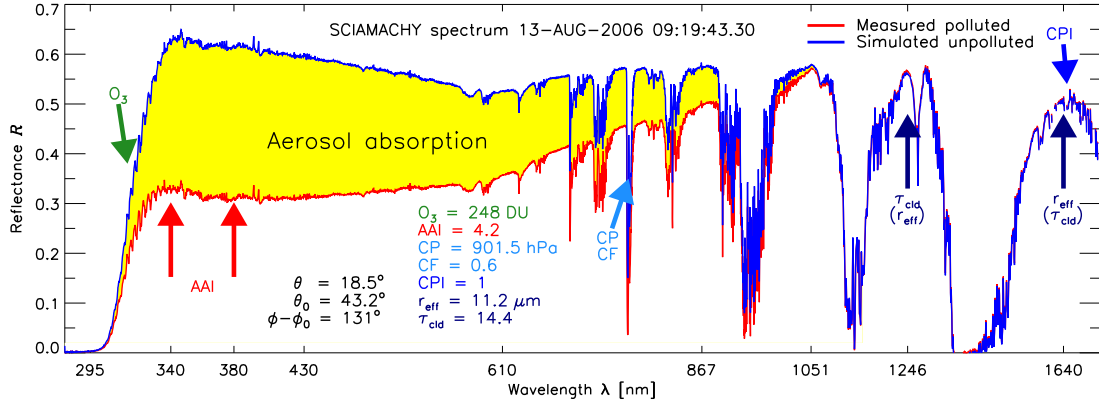
Figure 3. SCIAMACHY measured reflectance spectrum (red) on 13 August 2006, 09:19:43 UTC of the scene indicated by the arrow in Figure 5b; and the modelled equivalent unpolluted cloud reflectance spectrum (blue) for this scene. The difference between these two spectra (yellow, labelled 'Aerosol absorption') indicates the irradiance absorbed by the aerosols (see Figure 4). The parameters to model the cloud scene were retrieved at various parts of the spectrum (ozone (O3) between 325–335 nm, cloud fraction (CF) and cloud pressure (CP) at 760 nm, cloud phase index (CPI) around 1700 nm, cloud optical thickness (τ_{cld}) and effective radius (r_{eff}) at 1246 and 1640 nm). The AAI is retrieved from the reflectances at 340 and 380 nm [6].

tre thick layer using a gamma-distribution with effective radii varying between 4 and 16 microns and an effective variance of 1.5. This value is between typical values for stratus and stratocumulus [10]. Cloud Optical Thickness (COT) ranged from 2 to 48, and the height of the cloud bottom from 0 to 12 km. Only water clouds were modelled, which are the most likely ones encountered when aerosols overlie the cloud. However, the height of the clouds was not restricted to lower levels alone. The TOA reflectance was computed at a total number of $126^2 \times 19$ different geometries, which was scaled down to 36^2 solar and viewing angles and 19 azimuth angles. The surface albedo is accounted for analytically, by assuming it Lambertian and separating the contribution to the TOA reflectance from the surface and the atmosphere [cf. 11, 12]. In that case three surface albedo nodes suffice in the LUT. An example of the LUT is shown in Fig. 2. The LUT is searched using a linear interpolation of scene parameters retrieved from the measured reflectance spectrum.

3. APPLICATION TO SCIAMACHY

The algorithm is illustrated in Figure 3. The SCIA-MACHY reflectance spectrum observed on 13 August 2006, 09:19:43 UTC is shown in red. This is a typical measurement of a scene with smoke from the African continent that was advected over a marine low level cloud layer. The geometry for this scene was $[\theta, \theta_0, \phi - \phi_0] = [18.5°, 43.2°, 131.0°]$. The TOSOMI total ozone column Ω was 248 DU. The FRESCO cloud pressure and cloud fraction were 902 hPa and 0.6, respectively. The cloud droplet effective radius and cloud optical thickness, retrieved from the SWIR, were 11.2 μm and 14.4, respec-

tively. With these parameters an aerosol-unpolluted cloud reflectance spectrum was modelled, which is indicated by the blue curve. The measured and modelled spectra are close for wavelengths longer than 1246 nm, due to the assumption that the aerosol absorption optical thickness is negligible at these wavelengths. At wavelengths shorter than about 1100 nm, the reflectance spectra start to deviate, which is indicated by the yellow area. The difference increases with decreasing wavelength. This is caused by the aerosol absorption optical thickness, which increases with decreasing wavelength. At wavelengths below about 300 nm the differences disappear, because at these wavelengths the strong ozone absorption reduces the reflectance to zero. The aerosol absorption in the scene is confirmed by the high value of the AAI of 4.2.

The aerosol DRE over clouds for this scene was evaluated using equation (10). The various terms of this equation for the scene shown in Figure 3 are given in Figure 4 as a function of wavelength in the SCIAMACHY spectral range. The reflectance difference ($R_{cld} - R_{cld+aer}$) is given in Figure 4a, which is the same as the yellow area in Figure 3. It decreases with wavelength, except at those UV wavelengths where ozone absorption is so dominant that all radiation is absorbed. This term contains all the absorption effects in the scene which are not incorporated in the modelled cloud scene, and which are attributed to aerosol absorption. The anisotropy factor for the modelled cloud scene B_{cld} is not shown, but it is typically 0.8 - 1.0. The solar irradiance at TOA $\mu_0 F_0$ is given in Figure 4b. The total incident solar irradiance from $240 - 1750$ nm can be obtained by integrating the given irradiance spectrum and was 917 Wm^{-2}. The spectral irradiance change due to aerosol absorption ($E_{cld} - E_{cld+aer}$) can be obtained by combining these three terms according to equation (10), and is plotted in Figure 4c. By integrating over wavelength the total aerosol DRE over
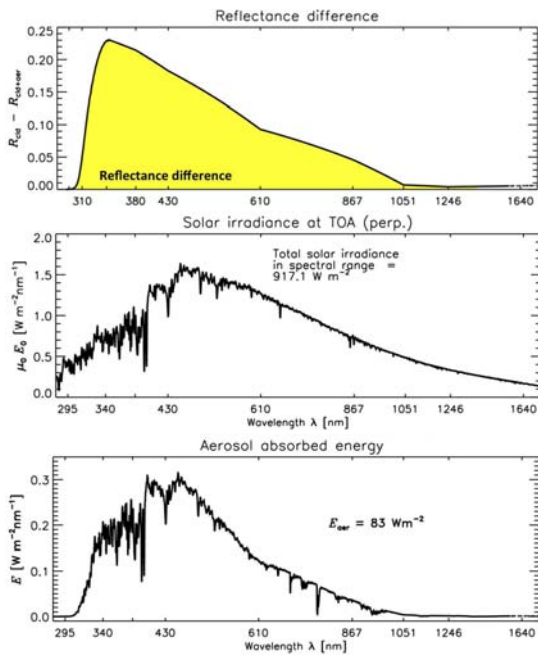
Figure 4. Various terms of equation (10) for the selected scene in Figure 5b. a) Reflectance difference between the blue and red curve in Figure 3. b) Incoming solar irradiance for this scene. c) Irradiance absorbed by the aerosols above the clouds.

clouds ΔE_{aer} was found to be 83 Wm^{-2} for this scene. Note that the spectral range of SCIAMACHY covers 92% of the solar energy spectrum, which is sufficient to capture the entire spectral aerosol DRE over clouds. The aerosol DRE becomes zero due to ozone absorption of the radiation below 300 nm and it also becomes zero for wavelengths longer than 1246 nm, assuming that the aerosol absorption has become negligible around that wavelength. The integration over SCIAMACHY's spectral range does not introduce an additional error as long as the aerosol absorption has become negligible around 1750 nm.

4. HORIZONTAL DISTRIBUTION

The retrieval of the aerosol DRE in cloudy scenes was tested during an episode of smoke over clouds over the South Atlantic Ocean. In August 2006 a two–week period of high AAI over clouds was observed over the South-Atlantic Ocean off the west coast of Namibia. These events can often be observed in this area from June to September, which is the local dry season. The high AAI values are caused by smoke from vegetation fires on the African mainland, which are advected over the Atlantic at altitudes of typically $1-5$ kilometres [e.g. 13, 14]. The horizontal distribution of aerosols is shown using the Absorbing Aerosol Index (AAI) from SCIA-MACHY (Fig. 5a). The AAI is retrieved in the UV from

the 340/380 nm pair [15, 13]. High AAI values are indicative of anomalous absorption in the UV, typically caused by UV–absorbing aerosols when ozone absorption is accounted for [16, 17, 12]. It has proved an excellent proxy to find aerosol polluted cloud scenes when combined with cloud fraction data [18, 19, 20]. The horizontal distribution of clouds is shown using MERIS RGB composites. MERIS is an imager on-board ENVISAT and provides excellent collocation with SCIAMACHY measurements. The vertical distribution of clouds and aerosols was provided by collocated CALIOP/CALIPSO measurements (not shown). Clearly, the horizontal distributions of aerosols and clouds are very variable, and change rapidly from day to day. The AAI shows a strong gradient and so does the aerosol DRE (Fig. 5b). Monitoring of the aerosol direct effect from passive instruments with daily global coverage will be highly advantageous for the understanding of aerosol–cloud interactions.

The aerosol DRE over clouds averaged for all cloudy scenes in the South Atlantic Ocean in August 2006 was was 23 ± 8 Wm^{-2} with a standard deviation during this month of 22 Wm^{-2} [21]. The maximum DRE over clouds in a SCIAMACHY pixel in August 2006 was 132 ± 8 Wm^{-2}.

5. CONCLUSIONS

The combination of space-based instruments provides unique opportunities for the quantification of aerosol direct radiative forcing, in order to further understand the climatic impact of anthropogenic and natural aerosols on climate. From SCIAMACHY/FRESCO+ data cloudy scenes can be determined and combining them with SCIAMACHY/AAI the global events of UV-absorbing aerosols over clouds becomes apparent. Furthermore, the entire radiance and irradiance spectrum in the UV, visible and near infrared is available from SCIAMACHY, providing the possibility to directly quantify the absorption and radiative forcing from the aerosols. The radiative forcing of UV-absorbing aerosols can be retrieved with high accuracy, using hyperspectral measurements and simulated clean cloud spectra.

REFERENCES

[1] J. Haywood and O. Boucher. Estimates of the direct and indirect radiative forcing due to tropospheric aerosols: A review. *Rev. Geophys.*, 38(4):513–543, 2000. 1999RG000078.

[2] U. Lohmann and J. Feichter. Global indirect aerosol effects: a review. *Atmos. Chem. Phys.*, 5, 2005.

[3] H. Yu, Y. J. Kaufman, M. Chin, G. Feingold, L. A. Remer, T. L. Anderson, Y. Balkanski, N. Bellouin, O. Boucher, S. Christopher, P. DeCola, R. Kahn, D. Koch, N. Loeb, M. S. Reddy, M. Schulz, T. Takemura, and M. Zhou. A review of measurement-based assessments of the aerosol direct radiative
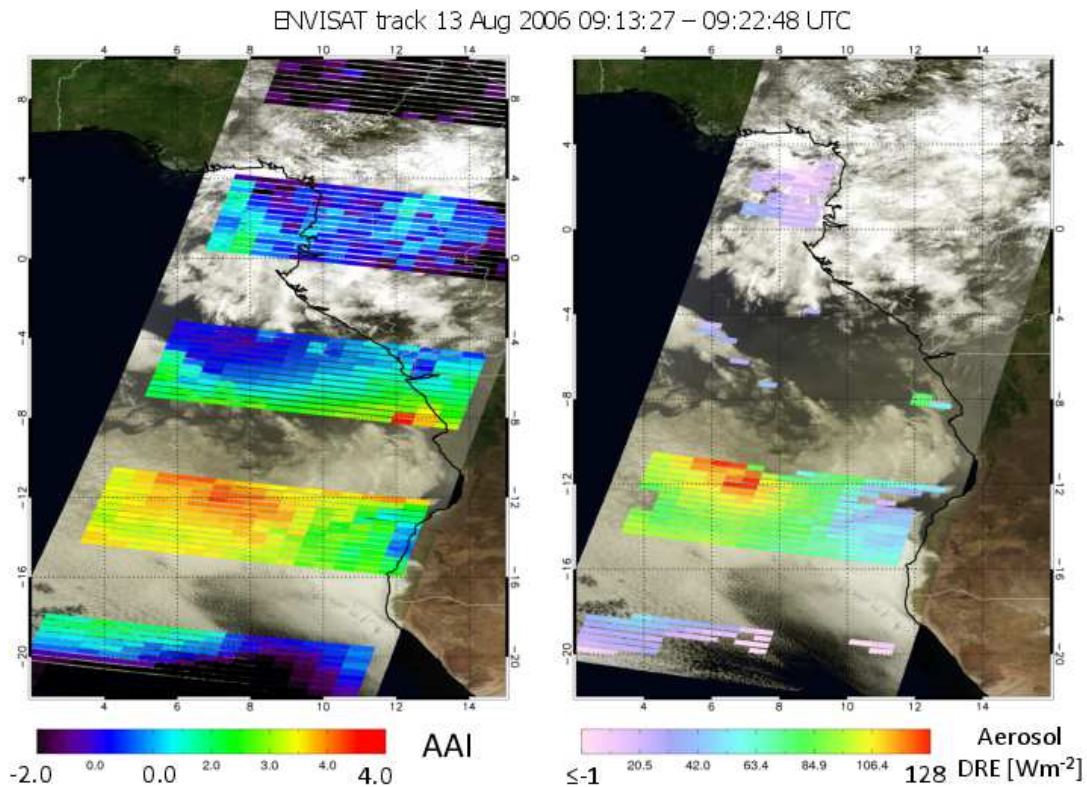
Figure 5. MERIS RGB image on 13 August 2006 from 09:13:27 – 09:22:48 UTC, overlaid with SCIAMACHY AAI values (same time) in he left panel and SCIAMACHY aerosol DRE in he right panel. Negative aerosol DRE values do not represent cooling effects by aerosol scattering and are not displayed.

effect and forcing. *Atmos. Chem. Phys.*, 6(3):613–666, 2006.

[4] P. Forster, V. Ramaswamy, P. Artaxo, T. Berntsen, R. Betts, D. W. Fahey, J. Haywood, J. Lean, D. C. Lowe, G. Myhre, J. Nganga, R. Prinn, G. Raga, M. Schulz, and R. Van Dorland. Contribution of working group I to the fourth assessment report of the intergovernmental panel on climate change. In S. Solomon, D. Qin, M. Manning, Z. Chen, M. Marquis, K.B. Averyt, M. Tignor, and H.L. Miller, editors, *Climate Change 2007: The Physical Science Basis.*, page 996. Cambridge Univ. Press, Cambridge, UK and New York, NY, USA, 2007.

[5] K. N. Liou. *An Introduction to Atmospheric Radiation.* Academic Press, 2002.

[6] L. G. Tilstra, M. de Graaf, I. Aben, and P. Stammes. In-flight degradation correction of SCIAMACHY UV reflectances and Absorbing Aerosol Index. *J. Geophys. Res.*, 117, 2012.

[7] P. Stammes. Spectral radiance modelling in the UV-visible range. In W.L. Smith and Y.M. Timofeyev, editors, *IRS 2000: Current problems in atmospheric radiation*, pages 385–388. A. Deepak Publishing, Hampton (VA), 2001.

[8] J. F. De Haan, P. B. Bosma, and J. W. Hovenier. The adding method for multiple scattering calculations of polarized light. *Astron. Astrophys.*, 183:371–391, 1987.

[9] G. P. Anderson, S. A. Clough, F. X. Kneizys, J. H. Chetwynd, and E. P. Shettle. AFGL atmospheric constituent profiles. Technical Report AFGL-TR-86-0110, Air Force Geophysics Laboratory, 1986.

[10] James E. Hansen. Multiple Scattering of Polarized Light in Planetary Atmospheres. Part II. Sunlight Reflected by Terrestrial Water Clouds. *J. Atmos. Sci.*, 28:1400 – 1426, 1971.

[11] S. Chandrasekhar. *Radiative Transfer.* Dover, Mineola, N.Y., 1960.

[12] M. de Graaf, P. Stammes, O. Torres, and R. B. A. Koelemeijer. Absorbing Aerosol Index: Sensitivity Analysis, application to GOME and comparison with TOMS. *J. Geophys. Res.*, 110, 2005.

[13] M. de Graaf, P. Stammes, and E. A. A. Aben. Analysis of reflectance spectra of UV-absorbing aerosol scenes measured by SCIAMACHY. *J. Geophys. Res.*, 112, 2007.

[14] M. de Graaf, L.G. Tilstra, I. Aben, and P. Stammes. Satellite observations of the seasonal cycles of absorbing aerosols in Africa related to the monsoon rainfall, 1995 - 2008. *Atm. Env.*, 44(10):1274–1283, 2010.

[15] M. de Graaf and P. Stammes. SCIAMACHY Absorbing Aerosol Index. Calibration issues and global results from 2002 – 2004. *Atmos. Chem. Phys.*, 5:3367–3389, 2005.

[16] J. R. Herman, P. K. Bhartia, O. Torres, C. Hsu, C. Seftor, and E. A. Celarier. Global distributions of UV-absorbing aerosols from NIMBUS 7/TOMS data. *J. Geophys. Res.*, 102:16,911–16,922, 1997.

[17] O. Torres, P. K. Bhartia, J. R. Herman, Z. Ahmad, and J. Gleason. Derivation of aerosol properties from satellite measurements of backscattered ultraviolet radiation: Theoretical basis. *J. Geophys. Res.*, 103:17,099–17,110, 1998.

[18] P. Stammes, L. G. Tilstra, R. Braak, M. de Graaf, and E. A. A. Aben. Estimate of solar radiative forcing by polluted clouds using OMI and SCIAMACHY satellite data. In *Proceedings of the International Radiation Symposium (IRS2008)*, pages 577–580. Foz do Iguaçu, Brazil, 2008.

[19] Karsten Peters, Johannes Quaas, and N. Bellouin. Effects of absorbing aerosols in cloudy skies: a satellite study over the atlantic ocean. *Atmos. Chem. Phys.*, 11:1393–1404, 2011.

[20] E. M. Wilcox. Direct and semi-direct radiative forcing of smoke aerosols over clouds. *Atmos. Chem. Phys.*, 12:139–149, 2012.

[21] M. de Graaf, L. G. Tilstra, P. Wang, and P. Stammes. Retrieval of the aerosol direct radiative effect over clouds from space–borne spectrometry. *J. Geophys. Res.*, 117, 2012.